The effects of averaging on the enhancement factor for absorption of light by carbon particles in micro-droplets of water

Vadim A. Markel

Department of Electrical Engineering, Washington University, Campus Box 1127, St. Louis, MO 63130-4899

Received February 15, 2001

Abstract

The effects of averaging of the enhancement factor for absorption of light by carbon particles inside water microdroplets are investigated numerically. A uniform distribution of carbon inclusions inside the water droplets is assumed. We perform the averaging over the size parameter of the droplet $x = 2\pi R/\lambda$ (R - radius of the droplet, λ - the incident wavelength) with different resolution in x.

1 Introduction

The absorption of electromagnetic radiation by carbonaceous soot aerosol is of considerable interest for climate and radiation energy transfer modeling [1–4]. The optical properties of free soot have been extensively studied [5–18]. In the visible and near IR, the first Born approximation [19] or the mean-field theory [20] provide accurate results for the absorptive properties of atmospheric soot. However, it is known that the soot often forms agglomerates with water microdroplets, especially in the clouds [1,21–24]. When a soot cluster is placed inside a water droplet, it is no longer excited by plane waves, but rather by internal modes of a high-quality optical resonator. To complicate things further, the resonator modes can effectively couple to the modes of clusters themselves. As a result, the absorption spectra of soot particles inside the microdroplets are very different from those of free soot.

The above fact stimulated a lot of interest in scattering and absorption by inhomogeneous spheres [25–39]. A brief review of theoretical results relevant to the topic of this paper can be found in [40]. The references [25–39] focus on a given incident light wavelength λ and the sphere radius R and, therefore, on a fixed size parameter $x = kR = 2\pi R/\lambda$. However, in most practical cases the microdroplets are polydisperse and excited by a broad-band radiation. This leads to a broad distribution of size parameters. In a recent paper [40] we have performed an averaging over the size parameter of microdroplets and studied the effects of narrow morphology-dependent resonances on the absorption enhancement factor. In particular, it was shown that the integral effect of these resonances is not small, and they should be accounted for in order to calculate the enhancement factor accurately. It was also shown that the enhancement factor averaged over a wide range of the droplet size parameters is a few times larger than for an off-resonant value of x. This increase was attributed to the integral effect of the morphology-dependent resonances.

However, the previous publication [40] lacked a systematic study of the dependence of the averaged enhancement factor on the resolution in x. This question is important since the averaging over size parameters is expected to yield the "true" result only for a sufficiently small step in x. In this paper, the results of such study are reported. It is shown that the averaged enhancement factor, calculated with fine resolution in x, is close to 25, which is even larger than previously reported in Ref. [40] (~ 14).

2 The enhancement factor

In this section we briefly summarize the results for the enhancement factor G and introduce relevant notations. Details of the derivations can be found in [18,40].

Our approach is based on a perturbation expansion which is mathematically similar to the approach used in [25,38]. The dielectric function of an inhomogeneous sphere is represented as a sum of a constant (unperturbed) value and a coordinate-dependent perturbation. The small parameter of the problem is the ratio of the volume of carbon inclusions, v, to the volume of the water droplet, $V = 4\pi R^3/3$. The absorption cross section of carbon inclusions inside the water droplet of radius R is given, to the first order in v/V, by

$$\langle \sigma_a \rangle = \frac{k \mathrm{Im} \epsilon_c}{|\mathbf{E_0}|^2} \int_V \langle \rho(\mathbf{r}) \rangle \, |\mathbf{E}_s(\mathbf{r})|^2 \, d^3\mathbf{r} \ , \tag{1}$$

where $\langle \ldots \rangle$ denotes averaging over the random realizations of carbon inclusions inside the water droplets, $\mathbf{E}_0$ is the amplitude of an incident plane wave, ϵ_c is the dielectric function of carbon, $\langle \rho(\mathbf{r}) \rangle$ is the average density of carbon inclusions normalized by the condition

$$\int_V \langle \rho(\mathbf{r}) \rangle d^3 r = v \tag{2}$$

and $\mathbf{E}_s(\mathbf{r})$ is the unperturbed internal field inside the sphere given by the expansion in terms of the vector spherical harmonics [41]:

$$\mathbf{E}_s = \sum_{n=1}^{\infty} i^n \frac{|\mathbf{E}_0|(2n+1)}{n(n+1)} \left(c_n \mathbf{M}_{o1n} - i d_n \mathbf{N}_{e1n}\right) \ . \tag{3}$$

Here c_n and d_n are the internal field Mie coefficients defined by

$$c_n = \frac{j_n(x)\left[x h_n^{(1)}(x)\right]' - h_n^{(1)}(x)\left[x j_n(x)\right]'}{j_n(x_1)\left[x h_n^{(1)}(x)\right]' - h_n^{(1)}(x)\left[x_1 j_n(x_1)\right]'} \ ; \tag{4}$$

$$d_n = \frac{j_n(x)\left[x h_n^{(1)}(x)\right]' - h_n^{(1)}(x)\left[x j_n(x)\right]'}{(x_1/x) j_n(x_1)\left[x h_n^{(1)}(x)\right]' - (x/x_1) h_n^{(1)}(x)\left[x_1 j_n(x_1)\right]'} \ ; \tag{5}$$

$$x = kR \ ; \quad x_1 = \sqrt{\epsilon_w} kR \ , \tag{6}$$

where ϵ_w is the dielectric function of water, $j_n(x)$ and $h^{(1)}(x)$ are the spherical Bessel and Hankel functions of the first kind, respectively, and the prime denotes differentiation with respect to the argument in parenthesis.

A few notes need to be made about formulas (1)-(6). First, the result (1) was obtained for a fixed wavelength λ and radius of the sphere R. However, it is averaged over random realizations of carbon inclusions. Thus the quantity $\langle \rho(\mathbf{r}) \rangle$ is defined as the *average* volume density and can be interpreted as the probability to find the point $\mathbf{r}$ inside the sphere to be occupied by carbon. It is natural to assume that this function is radially symmetrical: $\langle \rho(\mathbf{r}) \rangle = \langle \rho(r) \rangle$, while each *individual* realization $\rho(\mathbf{r})$ may not possess this property. Next, the water was assumed to be very weakly absorbing compared to carbon ($\mathrm{Im}\epsilon_w \ll \mathrm{Im}\epsilon_c$). This is a very accurate approximation in the visible and near-IR spectral regions. Apart from this assumption, and the requirement that the expansion parameter v/V is small, no other approximations were made. In particular, the size parameter of the sphere can be arbitrary.

Next we define the enhancement factor G as the ratio of the absorption cross section of carbon particles inside the water droplet and in vacuum :

$$G = \frac{\langle \sigma_a \rangle}{\langle \sigma_a^{(0)} \rangle} \ , \tag{7}$$

where $\langle \sigma_a^{(0)} \rangle = kv\mathrm{Im}\epsilon_c$ is the average absorption cross section of carbon soot in vacuum in the first Born approximation. It can be easily obtained from (1) by replacing the internal field $\mathbf{E}_s$ with a plane wave $\mathbf{E}_0 \exp(i\mathbf{k} \cdot \mathbf{r})$. Applying this definition to (1) we obtain

$$G = \frac{1}{v|\mathbf{E_0}|^2} \int_V \langle \rho(\mathbf{r}) \rangle \left| \mathbf{E}_s(\mathbf{r}) \right|^2 d^3\mathbf{r} \ . \tag{8}$$

Since the average density of carbon inclusions must be spherically symmetrical, we can write

$$G = \frac{1}{v|\mathbf{E_0}|^2} \int_0^R r^2 \langle \rho(r) \rangle dr \int \left| \mathbf{E}_s(\mathbf{r}) \right|^2 d\Omega \ . \tag{9}$$

Further, we use expansion (3) for $\mathbf{E}_s$ and, taking into account the mutual orthogonality of the VSHs, write the angular part of integral (9) as

$$\begin{aligned} \int \left| \mathbf{E}_s(\mathbf{r}) \right|^2 d\Omega = \sum_{n=1}^{\infty} & \frac{|\mathbf{E}_0|^2 (2n+1)^2}{n^2(n+1)^2} \\ & \times \left[|c_n|^2 \int |\mathbf{M}_{o1n}|^2 d\Omega + |d_n|^2 \int |\mathbf{N}_{e1n}|^2 d\Omega \right] \ . \end{aligned} \tag{10}$$

The angular integration can be performed directly using the normalization formulas for the VSHs, which yields

$$\begin{aligned} \int \left| \mathbf{E}_s(\mathbf{r}) \right|^2 d\Omega = 2\pi |\mathbf{E}_0|^2 \sum_{n=1}^{\infty} (2n+1) & \Bigg\{ |c_n|^2 j_n^2(k_1 r) \\ + |d_n|^2 \left[n(n+1) \left(\frac{j_n(k_1 r)}{k_1 r} \right)^2 + \left(\frac{j_n(k_1 r)}{k_1 r} + j_n'(k_1 r) \right)^2 \right] & \Bigg\} \ . \end{aligned} \tag{11}$$

Further calculations require specifying the form of $\langle \rho(r) \rangle$. In general, the distribution of carbon inclusions inside the microdroplets can be influenced by many factors such as the chemical composition of soot particles, surface tension forces, temperature, etc [42,43]. However, the average density of inclusions must be spherically symmetrical if there is no distinguished direction inside the sphere (we neglect gravity at this point). In this paper we consider the simplest case of a homogeneous distribution

$$\langle \rho(r) \rangle = v/V \quad \text{if} \quad r < R \ . \tag{12}$$

The case of a more general power-law distribution was considered in [18,40]. With the simple form (12) of $\langle \rho(r) \rangle$, the radial integrals in (9) can be calculated analytically. Then the final result for G becomes

$$G = \frac{3}{2x_1^3} \sum_{n=1}^{\infty} \left[\left(|c_n|^2 + |d_n|^2 \right) I(x_1) + |d_n|^2 x_1 j_n(x_1) \left(j_n(x_1) + x_1 j_n'(x_1) \right) \right] , \tag{13}$$

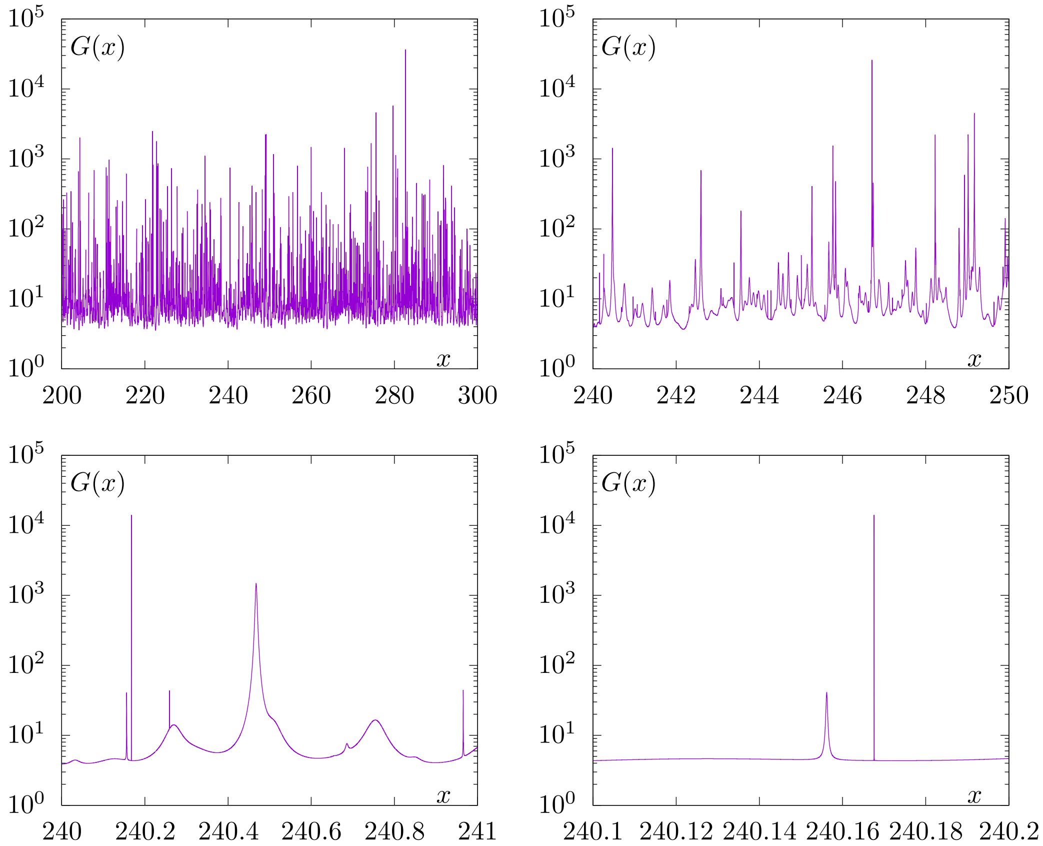

Fig. 1. Enhancement factor $G(x)$ as a function of x calculated with different resolution. Each plot contains $10,001$ points in x.

where

$$I(x_1) = \int_0^{x_1} x^2 j_n^2(x) dx = \frac{x_1}{2} \times \left[\left(x_1 j_n'(x_1)\right)^2 + x_1 j_n(x_1) j_n'(x_1) + \left(x_1^2 - n(n+1)\right) j_n^2(x_1) \right] . \qquad (14)$$

3 Results and discussion

We have calculated the function $G(x)$ in different intervals of x with different resolution. The results are shown in Fig. 1. Each plot contains $N = 10^4$ points in x. The first important feature that can be seen in these plots is the apparent absence of a systematic dependence on x (similar behavior was also observed in the interval $10 < x < 1000$ [40]). This leads to the conclusion that the results of averaging of $G(x)$ over x should not depend significuntly on the actual distribution over size parameters $p(x)$ which is determined by the distribution of droplets radiuses and by the spectrum of the incident light.

Second, as can be seen in Figs. 1c and 1d, the typical off-resonance value of

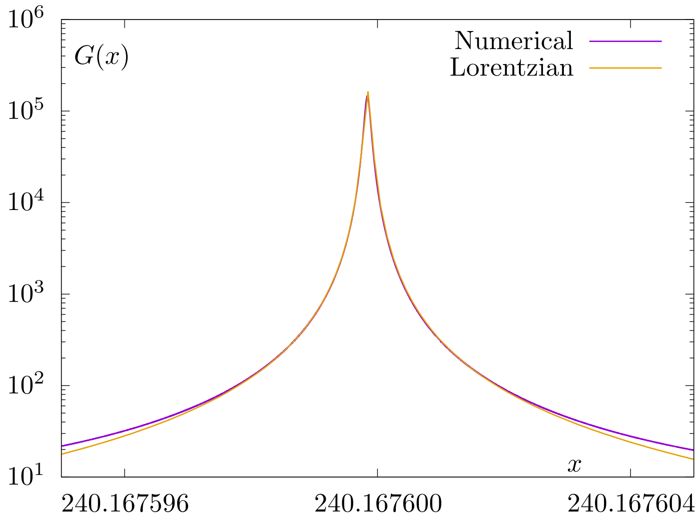

Fig. 2. Sharp resonance seen in Fig. 1c near $x = 240.17$ completely resolved. Approximation by a Lorentzian of the form $f(x) = w(\gamma/x_0)/((x - x_0)^2 + \gamma^2)$ is shown by the dashed line; the values of the parameters are $x_0 = 240.167599842$, $\gamma = 5 \cdot 10^{-8}$, $w = 2$.

G is approximately 5, which is close to the values previously reported [4,44]. However, the resonance values of G are extremely large. Some of the resonances are very narrow while the others are not. A completely resolved resonance with the half width $\sim 5 \cdot 10^{-8}$ is shown in Fig. 2. (The same resonance can be seen in Fig. 1d near $x = 240.17$ as a vertical line.) We also show in Fig. 2 an approximation of this peak by a Lorentzian.

Now we turn to averaging of $G(x)$ over x. The averaging was performed in different intervals $x \in [x_{min}, x_{max}]$ under the assumption that the distribution of droplets over size parameters is uniform in this interval. Therefore, the averaged value $\langle G \rangle$ is given by

$$\langle G \rangle = \frac{1}{N} \sum_{i=1}^{N} G(x_i) \ , \tag{15}$$

$$x_i = x_{min} + \Delta x (i - 1) \ , \quad \Delta x = (x_{max} - x_{min})/(N - 1) \ . \tag{16}$$

The results of such averaging are illustrated in Fig. 3 for different intervals $[x_{min}, x_{max}]$. It can be seen that, in all cases, the quantity $\langle G \rangle$ converges to well-defined constant value for sufficiently small Δx. This limiting value of $\langle G \rangle$ varies in the range $20 < \langle G \rangle < 25$, except in the interval $x \in [450, 550]$ (Fig. 3b), where $\langle G \rangle \approx 40$. The reason why $\langle G \rangle$ is anomalously high in this interval of size parameters is not clear; it can be attributed to appearance of a very strong resonance. In all cases, the averaged values of $\langle G \rangle$ can be seen to increase systematically (except for some very narrow peaks) as Δx decreases.

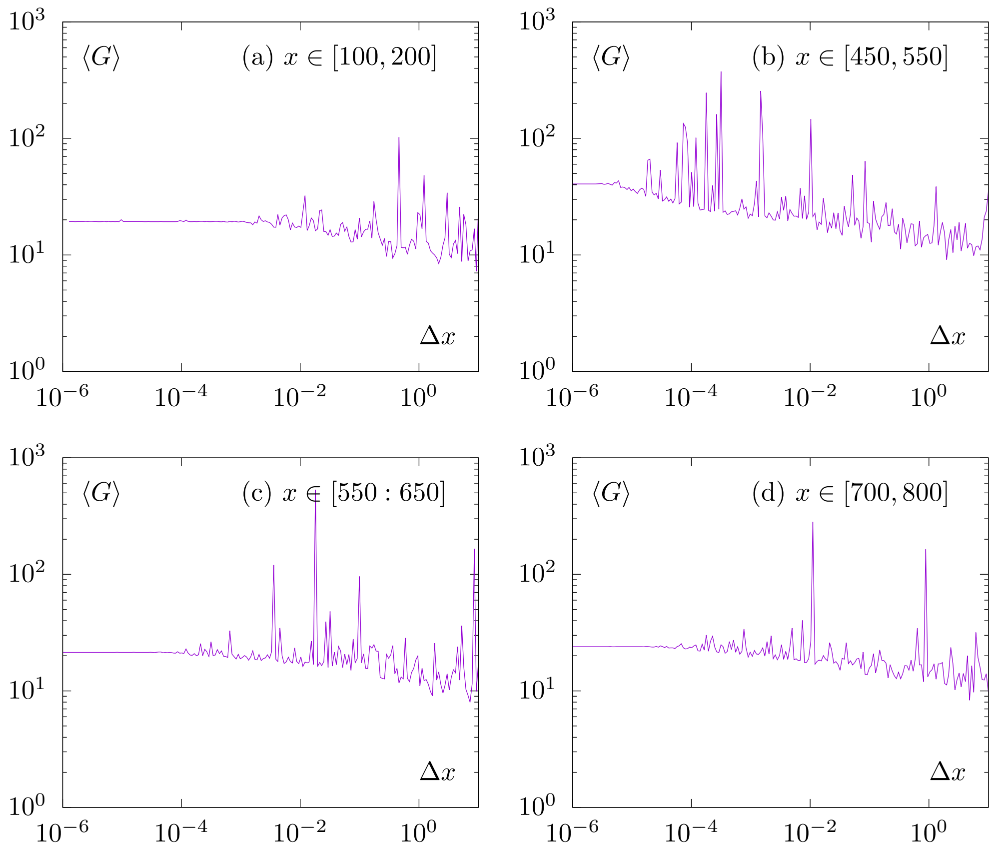

Fig. 3. $\langle G \rangle$ as a function of Δx for different averaging intervals $[x_{min}, x_{max}]$.

The most challenging numerical task is calculating $\langle G \rangle$ in a wide range of x. Similar to Ref. [40], we intend to average the enhancement factor for $x \in [10, 1000]$. For example, for $\lambda = 0.4\mu$m, this corresponds to the droplet radiuses in the range $0.64\mu\text{m} < R < 640\mu\text{m}$. (Study of smaller size parameters must be carried out separately, since there can be found a pronounced systematic dependence of $G(x)$ on x for $x < 10$.) The numerical complexity arises from the fact that $G(x)$ must be calculated at an extremely large number of points in this case. Note also that when x grows, calculation of $G(x)$ is more numerically complex, since the number of terms necessary for convergence of the series (13) grows approximately as x.

The results of the averaging of $G(x)$ in the interval $x \in [10, 1000]$ are shown in Fig. 4. Again, it can be seen that the averaged value of the enhancement factor converges to $\langle G \rangle \approx 25$ for $\Delta x \approx 10^{-6}$. However, this convergence is manifested not as strongly as in the smaller ranges of the size parameter (see Fig. 3). Continuing calculations for $\Delta x < 10^{-6}$ was numerically not feasible. Nevertheless, it appears evident that $\langle G \rangle$ is not smaller than at least 24, since $\langle G \rangle$ does not decrease below this value starting from $\Delta x < 10^{-4}$. Note also that in Ref. [40] we have calculated $\langle G \rangle$ for $\Delta x = 0.1$ and found $\langle G \rangle \approx 14$. As can be seen from Fig. 4, this value is, indeed, typical for $\Delta x \approx 0.1$. However, a

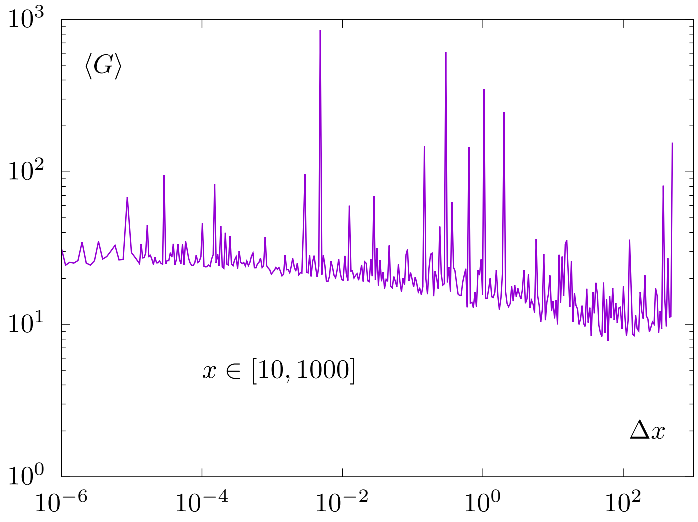

Fig. 4. $\langle G \rangle$ as a function of Δx for $x \in [10, 1000]$.

well manifested systematic increase of $\langle G \rangle$ can be seen as Δx decreases from 0.1 to 10^{-4} (apart from several high narrow peaks).

To conclude, we have found that the integral effect of the narrow morphology-dependent resonances on the enhancement factor G is not small. It leads to the increase of the averaged enhancement factor $\langle G \rangle$ by the factor of ~ 5 compared to the typical off-resonant value of $G(x)$.

Acknowledgements

This research was supported by Battelle under Contract DAAH04-96-C-0086. It was also partially supported by National Computational Science Alliance under Grant PHY980006N and utilized the NCSA HP/Convex Exemplar SPP-2000. The author is grateful to V. Shalaev and C. Bruce for very useful discussions.

References

[1] P. Chylek, V. Ramaswamy, R. J. Cheng, Effect of graphitic carbon on the albedo of clouds, J. Atmospheric Sci. 41 (21) (1984) 3076–3084.

[2] J. E. Penna, R. E. Dickinson, C. A. O'Neil, Effects of aerosol from biomass burning on the global radiation budget, Science 256 (?) (1992) 1432–?

[3] P. Chylek, J. Wong, Effect of absorbing aerosols on global radiation budget, Geophys. Res. Lett. 22 (8) (1995) 929–931.

[4] P. Chylek, G. B. Lesins, G. Videen, J. G. D. Wong, R. G. Pinnick, D. Ngo, J. D. Klett, Black carbon and absorption of solar radiation by clouds, J. Geophys. Res. 101 (D18) (1996) 23365–23371.

[5] R. D. Mountain, G. W. Mulholland, Light scattering from simulated smoke aggregates, Langmuir 4 (1988) 1321–1326.

[6] H. X. Zhang, C. M. Sorensen, E. R. Ramer, B. J. Olivier, J. F. Merklin, In sutu optical structure factor measurements of an aggregating soot aerosol, Langmuir 4 (1988) 867–871.

[7] H. Y. Chen, M. F. Iskander, J. E. Penner, Light scattering and absorption by fractal coagulations of smoke aerosols, J. Mod. Opt. 37 (2) (1990) 171–181.

[8] C. M. Sorensen, J. Cai, N. Lu, Test of static structure factors for describing light scattering from fractal soot aggregates, Langmuir 8 (1988) 2064–2069.

[9] U. O. Koylu, G. M. Faeth, Radiative properties of flame-generated soot, J. Heat Transfer 115 (1993) 409–417.

[10] U. O. Koylu, G. M. Faeth, Optical properties of overfire soot in buoyant turbulent diffusion flames at long residence times, J. Heat Transfer 116 (1994) 152–159.

[11] U. O. Koylu, G. M. Faeth, Optical propererties of soot in buoyant laminar diffusion flames, J. Heat Transfer 116 (1994) 971–979.

[12] N. G. Khlebtsov, A. G. Mel'nikov, Depolarization of light scattered by fractal smoke clusters: An approximate anisotropic model, Opt. Spectrosc. 79 (4) (1995) 656–661.

[13] D. W. Mackowski, Electrostatics analysis of radiative absorption by sphere clusters in the rayleigh limit: Application to soot particles, Appl. Opt. 34 (18) (1995) 3535–3545.

[14] T. L. Farias, M. G. Carvalho, U. O. Koylu, G. M. Faeth, Computational evaluation of approximate rayleigh-debye-gans/fractal-aggregate theory for the absorption and scattering properties of soot, J. Heat Transfer 117 (1995) 152–159.

[15] S. Manickavasagam, M. P. Menguc, Scattering matrix elements of fractal-like soot agglomerates, Appl. Opt. 36 (6) (1997) 1337–1351.

[16] C. M. Sorensen, C. Oh, P. W. Schmidt, T. P. Rieker, Scaling description of the structure factor of fractal soot composites, Phys. Rev. E 58 (4) (1998) 4666–4672.

[17] G. W. Mulholland, R. D. Mountain, Coupled dipole calculation of extinction coefficient and polarization ratio for smoke agglomerates, Combustion and Flame 119 (1-2) (1999) 56–68.

[18] V. A. Markel, V. M. Shalaev, T. F. George, Optics of Nanostructured Materials, Wiley series in lasers and applications, Wiley-Interscience, New York, 2000, Ch. Some theoretical and numerical approaches to the optics of fractal smoke, pp. 355–412.

[19] J. E. Martin, A. J. Hurd, Scattering from fractals, J. Appl. Cryst. 20 (1987) 61–78.

[20] M. V. Berry, I. C. Percival, Optics of fractal clusters such as smoke, Optica Acta 33 (5) (1986) 577–591.

[21] R. E. Danielson, D. R. Moore, H. C. Van Hulst, The transfer of visible radiation through clouds, J. Atmospheric Sci. 26 (1969) 1078–1087.

[22] H. Grassl, Albedo reduction and radiative heating of clouds by absorbing aerosol particles, Contrib. Atmos. Phys. 48 (1975) 199–210.

[23] S. Twomey, Computations of the absorption of solar radiation in clouds, J. Atmospheric Sci. 33 (1976) 1087–1091.

[24] K. Y. Kondratyev, V. I. Binenko, O. P. Petrenchuk, Radiative properties of clouds influenced by a city, Izvestia Akademii Nauk (USSR)- Fizika Atmosfery i Okeana 17 (2) (1981) 122–127.

[25] M. Kerker, D. D. Cooke, H. Chew, P. J. McNulty, Light scattering by structured spheres, J. Opt. Soc. Am. 68 (5) (1978) 592–601.

[26] F. Borghese, P. Denti, R. Saija, O. I. Sindoni, Optical properties of spheres containing a spherical eccentric inclusion, J. Opt. Soc. Am. A 9 (8) (1992) 1327–1335.

[27] M. M. Mazumder, S. C. Hill, P. W. Barber, Morphology-dependent resonances in inhomogeneous spheres: Comparison of the layered, J. Opt. Soc. Am. A 9 (10) (1992) 1844–1853.

[28] H.-B. Lin, A. L. Huston, J. D. Eversole, A. J. Campillo, P. Chylek, Internal scattering effects on microdroplet resonant emission structure, Opt. Lett. 17 (14) (1992) 970–972.

[29] P. Chylek, D. Ngo, R. G. Pinnik, Resonance structure of composite and slightly absorbing spheres, J. Opt. Soc. Am. A 9 (5) (1992) 775–780.

[30] D. Q. Chowdhury, S. C. Hill, M. M. Mazumder, Quality factors and effective-average modal gain or loss in inhomogeneous spherical resonators, IEEE J. Quantum Electron. 29 (9) (1993) 2553–2561.

[31] R. L. Armstrong, J.-G. Xie, T. E. Ruekgauer, J. Gu, R. G. Pinnik, Effects of submicrometer-sized particles on microdroplet lasing, Opt. Lett. 18 (2) (1993) 119–121.

[32] J.-G. Xie, T. E. Ruekgauer, R. L. Armstrong, R. G. Pinnik, Suppression of stimulated raman scattering from microdroplets by seeding with nanometer-sized latex particles, Opt. Lett. 18 (5) (1993) 340–342.

[33] J. Gu, T. E. Ruekgauer, J.-G. Xie, R. L. Armstrong, Effect of particulate seeding on microdroplet angular scattering, Opt. Lett. 18 (16) (1993) 1293–1295.

[34] F. Borghese, P. Denti, R. Saija, Optical properties of spheres containing several spherical inclusions, Appl. Opt. 33 (3) (1994) 484–493.

[35] K. A. Fuller, Morpology-dependent resonances in eccentrically stratified spheres, Opt. Lett. 19 (17) (1994) 1272–1274.

[36] K. A. Fuller, Scattering and absorption cross sections of compounded spheres. I. Theory for external aggregation, J. Opt. Soc. Am. A 11 (12) (1994) 3251–3260.

[37] D. Ngo, R. G. Pinnik, Supression of scattering resonances in inhomogeneous microdroplets, J. Opt. Soc. Am. A 11 (4) (1994) 1352–1359.

[38] S. C. Hill, H. I. Saleheen, K. A. Fuller, Volume current method for modeling light scattering by inhomogeneously perturbed spheres, J. Opt. Soc. Am. A 12 (5) (1995) 905–915.

[39] D. Q. Chowdhury, S. C. Hill, M. M. Mazumder, Absorptive bistability in a dielectric sphere, Opt. Comm. 131 (1996) 343–346.

[40] V. A. Markel, V. M. Shalaev, Absorption of light by soot particles in microdroplets of water, J. Quant. Spectrosc. Radiat. Transfer 63 (1999) 321–339.

[41] C. F. Bohren, D. R. Huffman, Absorption and Scattering of Light by Small Particles, John Wiley & Sons, New York, 1998.

[42] E. F. Mikhailov, S. S. Vlasenko, T. I. Ryshkevitch, A. A. Kiselev, Soot structure investigation: Adsorbtional properties, J. Aerosol Sci. 27 (1996) S709–S710, suppl. 1.

[43] E. F. Mikhailov, S. S. Vlasenko, A. A. Kiselev, T. I. Ryshkevich, Modification of carbon cluster fractal structure due to capillary forces, in: M. M. Novak, T. G. Dewey (Eds.), Fractal frontiers, World Scientific, Singapore, 1997, pp. 393–402.

[44] G. Videen, P. Chylek, Scattering by a composite sphere with an absorbing inclusion and effective medium approximations, Opt. Comm. 158 (1-6) (1998) 1–6.